E. Gazi[1]
J. Dwyer[1]
N. P. Lockyer[1]
J. Miyan[2]
P. Gardner[1]
C. Hart[3]
M. Brown[3]
N. W. Clarke[3]

[1] *School of Chemical Engineering and Analytical Science, The University of Manchester, Manchester M60 1QD, UK*

[2] *Department of Biomolecular Sciences, UMIST, P.O. Box 88, Manchester M60 1QD, UK*

[3] *Cancer Research UK, Paterson Institute, Christie Hospital NHS Trust, Manchester M20 4BX, UK*

Fixation Protocols for Subcellular Imaging by Synchrotron-Based Fourier Transform Infrared Microspectroscopy

Received 2 July 2004;
accepted 17 August 2004
Published online 23 November 2004 in Wiley InterScience (www.interscience.wiley.com).
DOI 10.1002/bip.20167

Abstract: *Synchrotron-based Fourier transform infrared (SR-FTIR) microspectroscopy is a powerful bioanalytical technique for the simultaneous analysis of lipids, proteins, carbohydrates, and a variety of phosphorylated molecules within intact cells. SR-FTIR microspectroscopy can be used in the imaging mode to generate biospectroscopic maps of the distribution and intensity profiles of subcellular biomolecular domains at diffraction-limited spatial resolution. However, the acquisition of highly spatially resolved IR images of cells is not only a function of instrumental parameters (source brightness, sampling aperture size) but also the cell preparation method employed. Additionally, for the IR data to be biochemically relevant the cells must be preserved in a life-like state without introducing artefacts. In the present study we demonstrate, for the first time, the differences in biomolecular localizations observed in SR-FTIR images of cells fixed by formalin, formalin–critical point drying (CPD), and glutaraldehyde–osmium tetroxide–CPD, using the PC-3 prostate cancer cell line. We compare these SR-FTIR images of fixed cells to unfixed cells. The influence of chemical fixatives on the IR spectrum is discussed in addition to the biological significance of the observed localizations. Our experiments reveal that formalin fixation at low concentration preserves lipid, phosphate, and protein components without significantly influencing the IR spectrum of the cell.* © 2004 Wiley Periodicals, Inc. Biopolymers 77: 18–30, 2005

Keywords: *synchrotron; infrared; subcellular imaging; fixation; prostate cancer*

Correspondence to: E. Gazi; email: E.Gazi@picr.man.ac.uk
Contract grant sponsor: EPSRC

INTRODUCTION

Fourier transform infrared (FTIR) spectroscopy is a powerful tool for the simultaneous analysis of a diverse range of biomolecules within intact cells, in vitro. This optically based, bioanalytical technique measures the transitions in vibrational modes (mainly stretching and bending) of the functional groups of biomolecules as a result of absorption and subsequent excitation by low-energy IR photons (0.05–0.5 eV). The functional group vibrations are representative of cellular constituents such as lipids, proteins, carbohydrates, and a variety of phosphorylated molecules that include nucleic acids. The resulting IR spectrum of the cell comprises a series of peaks as a function of the wavenumber that depict the state of chemical bonding, which includes intra- and intermolecular hydrogen bonding, van der Waals interactions, steric factors, and inductive or resonance effects. In addition, an indication of the relative intensities of various biomolecules within the cell can be readily obtained.

The integration of a microscope into the FTIR spectrometer enables it to be used in an imaging mode to create micron-scale chemical maps of a multicomposite sample such as that of a single cell. This can be achieved using a single point detector with an adjustable sampling aperture to define an area on the cell from which the spectral data can be acquired. The cell is then moved in small increments that complement the sampling aperture size, with an IR spectrum recorded at each increment, resulting in the IR chemical map. Thus, the lateral resolution of the IR map is defined by the sampling aperture size. However, biomolecules absorb IR radiation in the mid-IR range between 3300 and 650 cm^{-1} that corresponds to the wavelength range of 3 to $\sim$16 μm. Thus, for an aperture size of 5 $\times$ 5 μm, loss of signal is observed in the IR spectrum below 2000 cm^{-1}, which is a region where the majority of functional group vibrations arising from species within the cell absorb IR radiation. However, the reduction in signal to noise (S/N) imposed by aperture sizes near to or at the diffraction limit of light can be considerably improved using synchrotron (SR)-based IR radiation.

SR radiation is emitted from relativistic electrons as they are accelerated in a circular trajectory by magnets positioned around the circumference of an ultrahigh vacuum-insulated ring. The extracted beam has a cross-section of only a few hundred microns (or less) and encompasses the entire wavelength range of the electromagnetic spectrum. The mid-IR wavelengths (3–20 μm) of the SR source is subsequently focussed into a beam with a spot size of $\sim$10 μm and introduced as an external source into the FTIR spectrometer.[1] Thus, in comparison with a conventional laboratory IR source (blackbody radiator) that emits radiation in a 360° distribution, SR-IR radiation is of higher brilliance, since a greater number of photons are emitted per source area and solid angle. As a result, SR-IR radiation can deliver a relatively higher number of photons, compared to blackbody radiators, through a diffraction-limited sampling aperture, providing IR spectra with significantly higher S/N.[2]

In recent years, researchers have used imaging SR-FTIR microspectroscopy to demonstrate differences in the spatial distributions and intensity profiles of biomolecular domains within cells.[3,4] However, these SR-FTIR studies,[3,4] and previously reported blackbody-based IR cell imaging studies,[5,6] have analyzed cells after dehydration by air-drying and without fixation.

The aim of fixation is to preserve the structural and biochemical constituents of cells in as close to in vivo conditions as possible. There are two major consequences of analyzing cells without fixation. In the first instance, cells are naturally present in hydrated form, and the removal of intercellular water molecules, which are bound to macromolecules (proteins, phospholipids, and carbohydrates), can result in the collapse of internal structures, leading to the delocalization of biomolecular species. Air drying of cells causes delocalization of biomolecules as a result of large surface tension forces associated with the water–air interface passing through the cell. The removal of cells from pH-buffered growth medium and subsequent air-drying can also influence the osmotic pressure within these cells, resulting in cell shrinkage or swelling. The latter can cause membrane rupture and leaching of intercellular components. Secondly, fixation is necessary in cell biology because once cells are removed from the growth medium, the autolytic process begins unless prompt fixation is administered. Autolysis is a process whereby intracellular enzymes contained within lysosomes initiate the denaturing of proteins and dephosphorylation of mononucleotides, phospholipids, and proteins. Furthermore, autolysis involves chromatin compaction, nuclear fragmentation (involving RNA/DNA nucleases), and cytoplasmic condensation and fragmentation. Thus, in FTIR-based biomechanistic studies, where experimenters are interested in specific pathways of cellular biochemistry as a result of the cells' response to particular stimuli, the effects of autolysis as a consequence of inappropriate cell preparation may obscure these IR investigations.

The common methods of cell preservation involve chemical fixation or flash-freezing for subsequent freeze-drying. Flash-freezing is appropriate for cells

grown on substrates, which have good thermal contact with the freezing liquid medium and substrates that can withstand the low temperatures involved during the flash-freezing process. However, common substrates for FTIR experiments in transmission mode, such as CaF_2 or BaF_2 disks, will not suffice as these are too brittle and can snap under extreme temperatures. MirrIR plates (Kevley Technologies) can be used as culture substratum for reflectance mode FTIR experiments. However, in our group, systematic attempts at flash-freezing cells that have been cultured upon these substrates result in loss of cell integrity. This may be because these MirrIR plates are relatively thick (2 mm) and have a large thermal mass. Thus, the insulating effect of the MirrIR plate may slow down freezing rates and result in intercellular ice crystal formation during freezing. This can cause mechanical damage by rupturing cell membranes and lead to the discharge of cytoplasmic material into the extracellular matrix.

Researchers in the field of FTIR cell analysis have avoided chemical fixation due to the potential for interference of the fixative to the IR spectrum. Consequently, alternative methods of cell preparation have been employed. As mentioned earlier, air-drying can cause biomolecular delocalization and activation of cell autolysis. Thus, researchers have investigated the use of centrifugation as a method of dehydrating cells at a faster rate and to minimize air–water surface tension effects that occur during air-drying.[7] The centrifugation method of cell preparation was used to study, by FTIR, the response of cervical cancer cells to epidermal growth factor (EGF). The authors of this study[7] incubated their cells with EGF with increasing incubation times. They observed changes in protein conformation (noted by shifts in amide I peak position) as a result of phosphorylation by EGF (monitored by the peak area of the phosphate monoester vibration at 970 cm^{-1}), at consecutive time points. The results of this experiment[7] indicate that the centrifugation method of cell preparation is appropriate for studying phosphorylation of proteins in cells. However, its suitability for preserving the spatial locations of biomolecular domains for IR cell imaging studies has not been assessed.

Specialized equipment for maintaining live cells for in situ FTIR analysis has been investigated by Holman et al.[2] This incubator system sustains cell viability by maintaining a humidified environment, so as to retain a thin layer of growth medium around the cell during FTIR measurements. However, this method of maintaining live cells has not been assessed for long durations (>1 h), which are required for IR mapping experiments incorporating the single point detector configuration. Additionally, the cell would have to keep constant biochemistry during the time of IR image acquisition.

As well as cell fixation, the method of mounting cells onto the substrate for FTIR analysis is of importance. Jamin et al.[4] have analyzed cells deposited onto BaF_2 by cytospin. Cytospun cells are smaller and more spherical than cells cultured directly onto substrate. Since, in an IR cell imaging experiment, the IR beam is transmitted through the entire cell body, one might expect less localization of biomolecular domains in the resulting IR image of the cytospun cell due to greater overlay of cytoplasm above and below the nucleus as a consequence of the compact shape of the cell. In addition, imaging a smaller cell would require a smaller sampling aperture, which can reduce spectral information due to the diffraction limit of light. For example, Jamin et al.[4] used a 3×3 μm sampling aperture to achieve the spatial resolution required for their cytospun cells, which were $\sim$15 μm in diameter. However, S/N obtained at wavenumber of $\geq$1240 cm^{-1} using this aperture size was poor.

In the present study, we investigate the use of different chemical fixatives for obtaining biomolecular localisations in highly spatially resolved SR-FTIR biospectroscopic images of the prostate cancer cell line PC-3. First, we investigate the biomolecular localisations and intensity profiles in SR-FTIR images of cells that have been fixed in formalin (methanal). The common concentration of formalin used in cell biological preparations is 4% formalin in phosphate-buffered saline (PBS). Formalin is a coagulative protein fixative since it causes the crosslinking of the primary and secondary amine groups of proteins.[8] Formalin can also preserve lipids by the reaction of hydrated formalin (methylene glycol) with double bonds of unsaturated hydrocarbon chains.[9] The fixative action of formalin on lipids and proteins is reversible in the presence of water. Second, because the formalin fixative contains a significant amount of water, a postfixation technique will be administered in order to remove this water component from the cells, without surface tension effects. The postfixation technique to be investigated is critical point drying (CPD).[10] The CPD process involves several steps. First, the intercellular water molecules (from saline) in the prefixed cells must be displaced gradually with increasing concentrations of ethanol. The ethanol is then displaced by acetone, which is miscible with liquid CO_2. The acetone within the cells is then displaced by liquid CO_2, within a chamber. The chamber is heated with a simultaneous rise in pressure as liquid CO_2 enters the vapor phase. At a specific temperature and pressure, the density of the vapor equals the

density of the liquid, the liquid–vapor boundary disappears, and the surface tension is zero.

Thirdly, we shall investigate biomolecular localizations in SR-FTIR images of glutaraldehyde–osmium tetroxide (with CPD postfixation) fixed PC-3 cells. The aldehyde groups of glutaraldehyde can react with the amino groups of proteins to form imines in an irreversible reaction. The commonly used postfixative to glutaraldehyde is osmium tetroxide (OsO_4), which can preserve lipids by the formation of cyclic esters and is also an irreversible reaction.[8] CPD glutaraldehyde–osmium tetroxide fixed cells preserves fine structure as observed in electron microscopy studies[11]; therefore, although chemically the most invasive, they should provide the benchmark for spectral localization.

Finally, we shall compare the biomolecular localizations in SR-FTIR images of cells that are fixed using the above-mentioned protocols, with unfixed cells that have been prepared by a previously reported centrifugation method.[7]

METHODS AND MATERIALS

PC-3 Cell Line Culture on MirrIR Substratum

The PC-3 cell line was cultured upon nontoxic MirrIR (Kevley Technologies, Chesterland, Ohio) substrates (sterilized in absolute ethanol for 1 h). The PC-3 cell line was cultured in Ham's F12, 7% Fetal Calf Serum (FCS), and 2 m*M* L-glutamine.[12] Cultures were grown at 37°C in a humidified atmosphere of 5% CO_2 in air. All reagents were purchased from Sigma–Aldridge, Poole, UK. All tissue culture media were obtained from Invitrogen, Paisley, UK.

Cell Fixation

Formalin-Fixed Cells. MirrIR slides, 3 days' postseeding with PC-3 cells, were removed from growth medium and fixed in 4% formalin in PBS for 20 min at room temperature. These cells were then briefly washed in distilled water for 3 s to remove the residue PBS from the surface of the cells. The cells were dried under ambient conditions and stored in a desiccator until FTIR analysis.

CPD of Formalin-Fixed Cells. The PC-3 cell line was removed from growth medium and fixed in 4% formalin in PBS. The aqueous component of the formalin–PBS fixative was replaced by ethanol through 5-min immersions in 50% ethanol, 70% ethanol, 90% ethanol, and 100% ethanol. Ethanol was then replaced with cold acetone (10-min immersion). The cell line was quickly loaded into the CPD chamber. The inlet valve was opened to allow liquid CO_2 to fill the chamber $\frac{3}{4}$ full. The cell line was immersed for 15 min for the acetone–liquid CO_2 mixture to equilibrate and then flushed out. This step was repeated twice more to substitute all the acetone with liquid CO_2. Phase transition was then induced by heating the chamber to 45°C with a pressure of 108 bar. At this point the liquid–air interface disappears and the cell line is left in a preserved state (assessed under a high-power optical microscope). The cell line was removed from the chamber and stored in a desiccator until FTIR analysis.

Glutaraldehyde–Osmium Tetroxide–Critical Point Dried Fixed Cells. All of the chemicals used in the following procedure were kept cold (4°C). The PC-3 cells were removed from culture media and immediately fixed for 2 h in 2.5% glutaraldehyde in 0.1*M* sodium cacodylate in 2 m*M* $CaCl_2$, pH adjusted with HCl to 7.3–7.4. Cells were subsequently washed in 2 m*M* $CaCl_2$ and 0.1*M* sodium cacodylate in distilled water for 10 min. This step minimized the presence of unreacted polymerized glutaraldehyde, which can react with osmium tetroxide (during postfixation) to produce small black spots on the final specimen. Postfixation was carried out for 20 min in 1:1 osmium tetroxide 2% stock in 0.2*M* sodium cacodylate with 4 m*M* $CaCl_2$, resulting in a final concentration of 1% osmium tetroxide in 0.1*M* sodium cacodylate with 2 m*M* $CaCl_2$. The cells were then washed in 0.1*M* sodium cacodylate in 2 m*M* $CaCl_2$ in distilled water for 10 min to remove excess osmium tetroxide. The cells were CPD using the same protocol as described earlier in the section immediately above.

Unfixed Cells. A sample protocol devised by Tobin et al.[7] was used to prepare the unfixed cells. The PC-3 cells were removed from growth medium and washed twice with PBS and then centrifuged for 5 min at 180× *g*, followed by air-drying. The cells were stored in a desiccator until FTIR analysis.

Preparation and FTIR Analysis of Reference Fixative Chemicals

A formalin solution (~38 weight % in water) containing ~10% methanol stabilizer and glutaraldehyde solution (25 weight % in water) was pipetted onto MirrIR slides for FTIR analysis. Both chemicals were obtained from Sigma–Aldrich, UK. Formalin and glutaraldehyde were analyzed in reflection mode using the Nicolet Magna system 550 spectrometer. FTIR spectra were obtained in the spectral range between 4000 and 750 cm^{-1} at 4 cm^{-1} resolution with 512 coadded scans.

SR-FTIR Microspectroscopic Cell Imaging

SR-FTIR spectral maps of the PC-3 cell lines were collected at the Daresbury Laboratory synchrotron radiation source (SRS) using beamline 11.1. For this, a Nicolet Nicplan IR spectrometer, equipped with a liquid nitrogen cooled Mer-

cury Cadmium Telluride/A (MCT/A) detector and a potassium bromide (KBr) beam splitter, was used in reflectance mode. FTIR area maps of the PC-3 cell were collected with a 7×7 μm aperture sampling aperture at a 3-μm step size. The choice of aperture size was based on work by Holman et al. who measured S/N ratios as a function of aperture size.[2] The S/N ratio value of aperture sizes less than 10 μm decreases dramatically from approximately 20,000 at 10 μm to 250 at 5 μm, due to diffraction limitations. In the present study, we found that an aperture size of 7×7 μm with 3-μm step size was a good compromise between obtaining spectral information with good S/N down to 1000 cm^{-1} and providing adequate spatial resolution for resolving biomolecular domains in the SR-FTIR image of the cell.

A background was recorded after every 10-sample spectra to correct for water vapor differences during the course of the mapping experiment and differences in the SR beam current. Optical images of these cell lines were obtained at 320× magnification (32×objective, 10× eyepiece).

Histochemistry

Following FTIR measurement, cell membrane integrity was assessed using trypan blue staining. A 1:1 trypan blue : PBS solution was pipetted onto the specimen slide and a coverslip was placed above. Cells that have lost membrane integrity absorb trypan blue and appear blue, whereas cells that have retained membrane integrity do not. These images were captured using a Leica DM LB microscope.

Data Processing

FTIR spectra of formalin and glutaraldehyde were baseline corrected with OMNIC v.6.2 software. The SR-FTIR cell images were processed with Atlμs. This software permits an area map collected with isolated data points to be filled. The fill procedure adds between each data point the number of interpolated data points specified by the fill level. This increases the number of contours in the displayed contour map, making the change in contour value from one location to another appear more gradual and smoothing the edges of shapes in the map. All SR-FTIR area maps were processed with a fill level of 6, since initial processing of the SR-FTIR images revealed that fill levels of 2–8 did not significantly alter the intensity distributions of the functional group vibrations in a way that would alter any biological interpretations reported in this study. The OMNIC software permitted the baseline corrected areas of selected peaks to be mapped across the image. Overlays of different peak intensity SR-FTIR images were processed with Jasc Paint Shop Pro v.7.

RESULTS AND DISCUSSION

SR-FTIR Images of Formalin-Fixed PC-3 Cell Line

PC-3 cells, cultured upon MirrIR plates, were fixed in 4% formalin in PBS and subsequently rinsed for 3 s in deionized water. This was found to be an important step to remove residual PBS from the surface of the cells. Figures 1a and b compare optical images of formalin-fixed cells with and without the water rinse step. A clear distinction can be made between the nuclear and cytoplasmic compartments in cells that are rinsed in deionized water (Figure 1b).

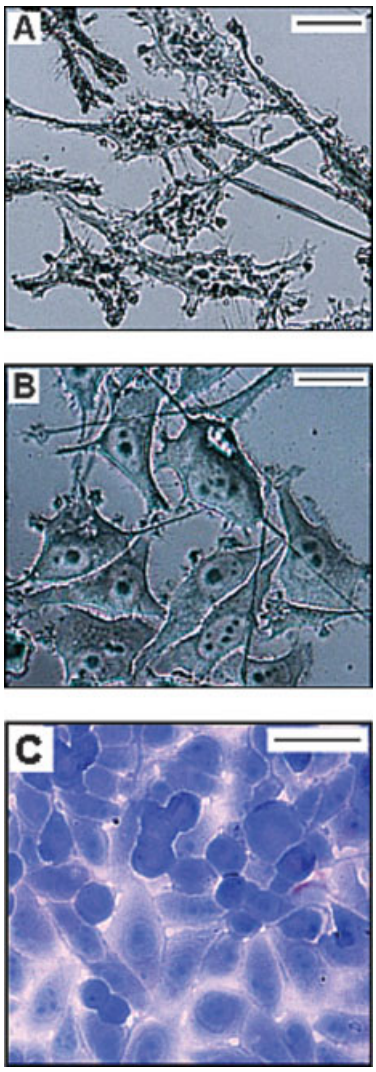

FIGURE 1 Photomicrographs of formalin-fixed PC-3 cells (same magnification) (a) without subsequent rinsing in deionized water and (b) with 3-s rinse in deionized water to remove residue PBS from the surface of the cells. (c) Formalin-fixed PC-3 cells are positive to trypan blue staining, indicating some loss of membrane integrity. Scale bar in all photomicrographs = 50 μm.

The trypan blue stain was used to assess the membrane integrity of the formalin-fixed cells. The cells were found to be positive to trypan blue staining, indicating some loss of plasma membrane lipids (Figure 1c). The loss of membrane lipids may be due to

the chemical mechanism involved during formalin fixation of lipids, which is reversible in the presence of water.

An optical image of a formalin-fixed PC-3 cell is shown in Figure 2a. The nucleus is visible with a circular border and is located at the centre of the cell body. A prominent nucleolus (DNA–histone protein complex) is observed at the center of this nucleus. The cytoplasmic compartment of the cell is located on either side of the nucleus. SR-FTIR images of the intensity distributions of various biomolecules, as depicted by their representative vibrational modes, are presented in Figures 2b–e. Figure 2g compares SR-FTIR spectra taken from the nucleoli, a region of nuclear lumen–organelle overlap (explained within the following text) and cytoplasm. We observe good S/N within the spectral range of interest (3000–1200 cm^{-1}) in each of these spectra.

The intensity distribution of the amide I peak across the PC-3 cell is shown in Figure 2b. The amide I peak shows intense absorption (white pixels) originating from the prominent nucleolus at coordinates (33 and 12 μm). This intense absorption arises from the amide functional group of the histone proteins as well as from the C═O stretch of nucleic acids within DNA,[13] which are bound to these histones. The C═O functional group vibration of nucleic acids does not overlap with the amide II peak.[13] Hence, we observe intense localization of amide II within the cytoplasm (Figure 2c), which suggests that it is associated with synthesized proteins. The correlation of the amide II vibrational mode with synthesized proteins has also been made by Diem et al.[14] It must be noted at this juncture that the intensity distribution of the amide II peak area, presented in Figure 2c and other amide II images of the cells reported in this study, were processed after baseline correction between the spectral region 1578 and 1482 cm^{-1} and not between 1730 and 950 cm^{-1} as for other peaks (amide I and phosphate) shown in Figure 2g. We find that the intensity distribution of the peak area of the amide II band as a result of baseline correction between 1730 and 950 cm^{-1} yielded a similar localization to that observed for the amide I peak area. However, the distribution of the amide II peak area, subsequent to integration using the spectral range of 1578–1482 cm^{-1}, gave rise to an intensity profile that may be attributed to metabolic proteins within the cytoplasm (Figure 2c). This observation was replicated in other SR-FTIR images of cells processed in the same manner (see Figure 6c). As mentioned above, the valley in between the amide I and amide II peaks has contribution from the C═O functional group vibration of nucleic acids.[13] Thus, in Figure 2g we observe that the valley

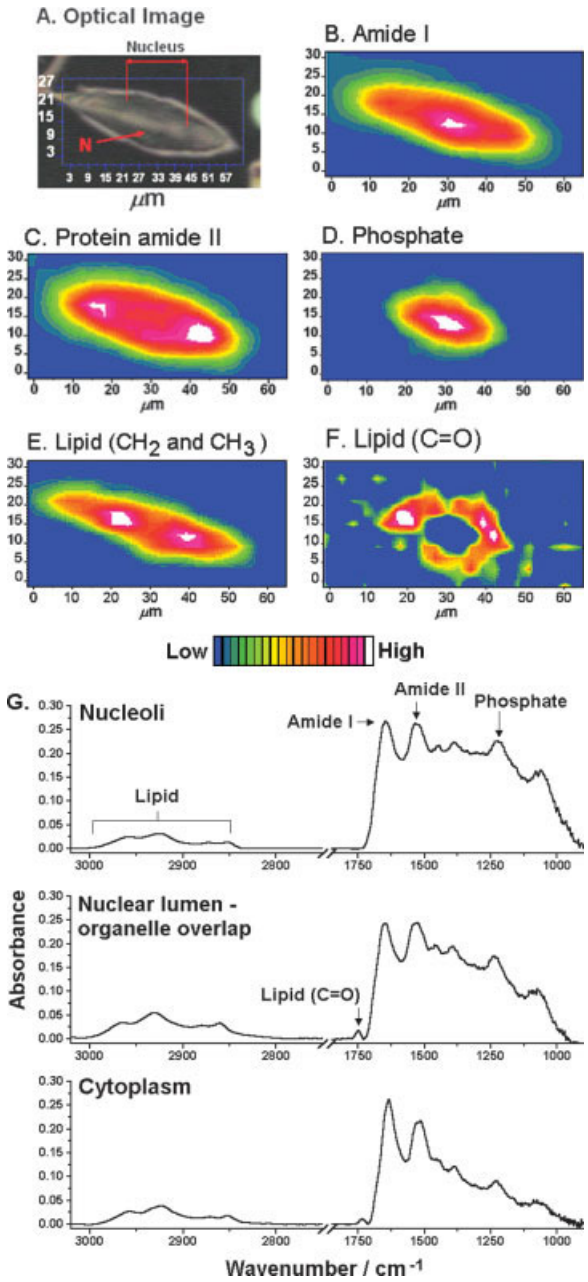

FIGURE 2 (a) Optical image of a single, formalin-fixed PC-3 cell. The cells nucleus and nucleolus (N) are identified. Localizations and intensity profiles of (b) amide I (1708–1569-cm^{-1} peak area); (c) protein amide II (1562–1475-cm^{-1} peak area); (d) phosphate (1280– 1174-cm^{-1} peak area); (e) lipid CH_2 and CH_3 (3000–2830-cm^{-1} peak area); (f) lipid ester (C═O) (1752– 1722-cm^{-1} peak area). IR image recorded with a 7 × 7-μm sampling aperture at a 3-μm step size. Image acquisition time was 6 h and 27 min. (g) IR spectrum of the nucleoli [taken from coordinates (30 and 14 μm)], a region of nuclear lumen–organelle overlap [taken from coordinates (20 and 15 μm)] and cytoplasm [taken from coordinates (15 and 18 μm)].

between the amide I and II peaks is deeper in the IR spectrum derived from the cytoplasm where there is no contribution from nucleic acid absorption, when compared with the IR spectrum derived from the nucleoli or region of nucleoli–organelle overlap, in which there is a large contribution of nucleic acid absorption at this spectral region. Consequently, we suggest that baseline correction between ~1578 and 1482 cm^{-1} provides a better depiction of the amide II intensity profile.

The most intense absorption from phosphate [$\nu_{as}(PO_2)$] (Figure 2d) arises in the nucleolus and colocalizes in the region of intense amide I absorption. The intense phosphate absorption at this location is derived from the sugar phosphate backbone of DNA. The slightly lower intensity of phosphate (red-pink pixels) distribution within the nuclear lumen may arise from nucleic acids of RNA that serve as intermediate communicators between DNA in the nucleus and ribosomes on the rough endoplasmic reticulum (ER) for protein synthesis.

Figure 3b demonstrates that the most intense absorptions arising from the asymmetric and symmetric lipid acyl chain (CH_2 and CH_3) vibrations (see Figure 2e for single-peak-extracted image) are located at the nucleus–cytoplasm interface and partially extend into the nuclear region (yellow pixels). The most intense signals arising from the lipid ester-stretching (C═O) mode are also localized at the lipid- (CH_2 and CH_3) occupied regions of the cell (Figure 3b). However, the slightly lower intensity of the lipid ester (C═O) (red-orange pixels) provides a distinct hemispherical shape around the nucleus (see Figure 2f for single-peak-extracted image). The localizations and intensity distributions of the lipid vibrations suggest that they arise from the membranes of cytoplasmic organelles and may be tentatively assigned to organelles such as the ER and Golgi apparatus. The hemispherical shape and cytoplasmic position (near to the nucleus) of both of these organelles support those observed in scanning electron microscopy and fluorescent imaging studies.

The region of lipid (CH_2 and CH_3) and (C═O) absorptions that extends into the nucleus may indicate overlap of organelles that occupy cytoplasmic material above and below the nucleus. This is diagrammatically represented in Figure 3a as zone 2, in which IR light passes through cytoplasmic organelles as well as the nucleus. However, in zone 3, cytoplasmic material above and below the nucleus is at a minimum. Consequently, the concentration of organelles at zone 3 is lower than in any other zones. Thus, in zone 3, IR light is transmitted primarily through the nucleus and nucleolus. This may explain the depression in lipid signal at this location in the SR-FTIR image of the

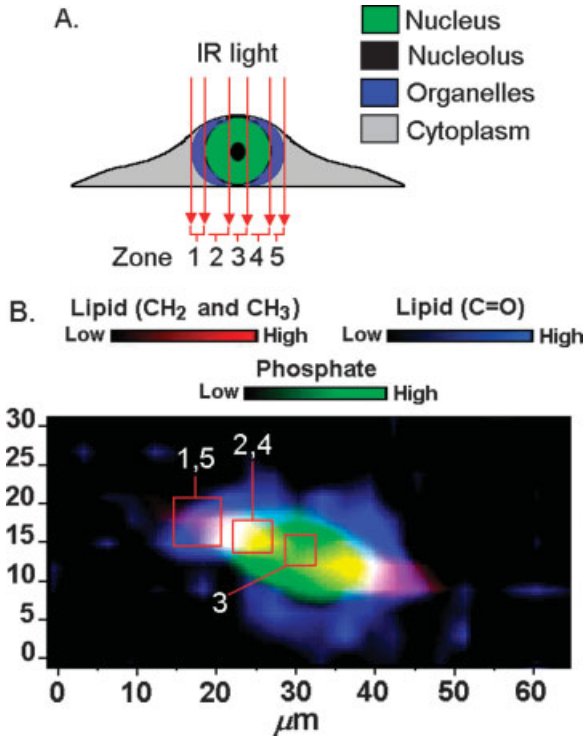

FIGURE 3 (a) A diagrammatic representation of the side profile of the PC-3 cell analyzed by SR-FTIR. IR light transmits through different cellular components in the cells body. Zones 1 and 5 represent transmission of IR light through cytoplasmic organelles only. Zone 2 and 4 represent transmission of IR light through the nucleus and organelles. Zone 3 represents transmission through nucleus and nucleolus. (b) SR-FTIR overlay image of the intensity distributions corresponding to the phosphate (1280– 1174-cm^{-1} peak area) and lipid (C═O) domains within the PC-3 cell. These localizations depict subcellular structures corresponding to the nucleus (phosphate) and cytoplasmic organelles (lipid ester C═O, CH_2, and CH_3; ER, Golgi apparatus, mitochondria, and lysosomes). The boxed locations represent examples of the different zones (1–5) described in (a).

PC-3 cell (Figures 2e,f and 3b). In Figure 3a, zones 1 and 5 represent transmission of IR light through cytoplasmic organelles that are situated beside the nucleus. In this region, the intensity of phosphate signal drops (yellow-green pixels in Figure 2d), since the nucleus is no longer in the path of the IR light, while the lipid signals exhibit an increase in intensity due to a greater concentration of cellular organelles. Examples of each of these zones have been designated in the SR-FTIR overlay image in Figure 3b.

The lower intensity of phosphate distribution (yellow-green pixels in Figure 2d) surrounding the nucleus is colocalized in regions occupied by intense lipid ester (C═O) absorption. This may be indicative of phosphorylation processes occurring within or-

ganelles such as the ER, which is in continuity with the nuclear envelope. For example, protein biosynthesis occurs in the ER[15] and can be recognized from the SR-FTIR image by intense localization of amide II absorptions [at coordinates (20 and 15 μm) and (40 and 13 μm) in amide II image, Figure 2c] in regions of intense lipid ester (C═O) signal (white pixels in Figure 2f). The ER also plays a central role in phospholipid synthesis, which involves the utilization of phosphorylated molecules such as glycerol-3-phosphate and phosphatase.[15]

The slightly lower intensity of the lipid ester (C═O) signal (depicted by orange pixels in Figure 2f) that colocalizes with the low phosphate signal around the nucleus and does not colocalize with the high amide II signal may be indicative of phosphorylation processes within organelles such as the Golgi complex, lysosomes, and mitochondria.

It is important to note that the overall phosphate and lipid distribution across the cell is indicative of intercellular lipid and phosphate domains. This is because the relatively low spatial resolution of the IR technique does not permit resolution of the less common domains within the plasma membrane bilayer, such as carbohydrates and proteins. Thus the intensity of absorption arising from the plasma membrane is mainly due to phospholipids, which represent the most common biomolecule in the plasma membrane. Hence, the phospholipids in the plasma membrane can be considered as a constant across the whole cell. Consequently, the heterogeneity of absorption intensities of phosphate and lipid signals and their localizations reflects absorption arising from additional phosphate and lipid domains within the cytoplasm of the cell.

In addition, it is noteworthy to mention that if the thickness of the cell was the overriding factor determining the apparent localization of molecules in Figures 2b–f, then we would expect to see a series of concentric rings radiating from the nucleus of the cell. However, this is not the case, since the intensity distributions across the cell for different regions of the spectrum are very different. However, we acknowledge that there may be some influence of cell thickness to the images presented in this study. One might expect that the nucleus, located at the center of the cell (Figure 2a), would exhibit enhanced intensities of molecular functional group vibrations due to the increased path length of the IR beam through the cell at that location (see Figure 3a, zone 3). Similarly, the intensity of molecules located at the periphery of the cell would be expected to be somewhat suppressed due to a shorter path length at this point. Accepting this, it is clear that our data still reveal localization, which can be correlated with known cellular biology. Note that it is standard practice in IR spectroscopy to account for the difference in sample thickness by normalizing to a common IR peak in the spectrum. However, this is only applicable if that peak is homogeneously distributed throughout the sample. In the case of a cell, no such band exists; thus, normalization cannot be achieved.

The influence of formalin absorption on the localizations of IR vibrational modes arising from the cells constituents is not apparent from the images presented in Figure 2. This is now discussed in further detail. In Figure 2g, typical IR spectra derived from the nucleoli and cytoplasm of the formalin-fixed PC-3 cell are shown. Figure 4a shows the IR spectrum of formalin, which contains methanol (~1%) to prevent polymerization. Peaks in the IR spectrum of formalin may overlap with bands arising from the acyl chain of cellular lipids (~2840– 2794 cm^{-1}), amide I (~1645 cm^{-1}), phosphate (~1240 cm^{-1}), and several other functional group vibrations arising from biomolecules below 1115 cm^{-1}.

The most intense peak in the spectrum of formalin occurs at 1000 cm^{-1}. Thus, the intensity of absorption at 1000 cm^{-1} in the spectrum of the cytoplasm and nucleoli from the formalin-fixed cell (Figure 2g) can be considered as the upper limit of formalin absorption. The intensity of absorption at 1000 cm^{-1} in the spectrum derived from the cytoplasm and nucleoli of the formalin-fixed cell is 0.015 and 0.07 AU, respectively. Therefore, the formalin spectrum can be normalized to each of these values and subtracted from the spectrum of the nucleoli and cytoplasm shown in Figure 2g. Figures 4b and c show the overlay of each of these spectra before and after this formalin subtraction. Negligible differences in the intensities of peaks across each spectrum is observed in the wavenumber range 3000–1100 cm^{-1}.

Additionally, although the trypan blue stain showed loss of plasma membrane lipids (Figure 1c), this may have not resulted in significant loss of cytoplasmic components since the localizations of functional group vibrations observed in the SR-FTIR images can be explained in terms of fundamental biology.

SR-FTIR Images of the Formalin–CPD Fixed PC-3 Cell Line

The CPD process of cell preservation is used in this study to remove the water component from formalin-fixed PC-3 cells without surface tension effects. The CPD protocol used here exposes cells to three chemical steps before applying CPD. First, the cells were fixed in a formalin–PBS solution. Second, a series of

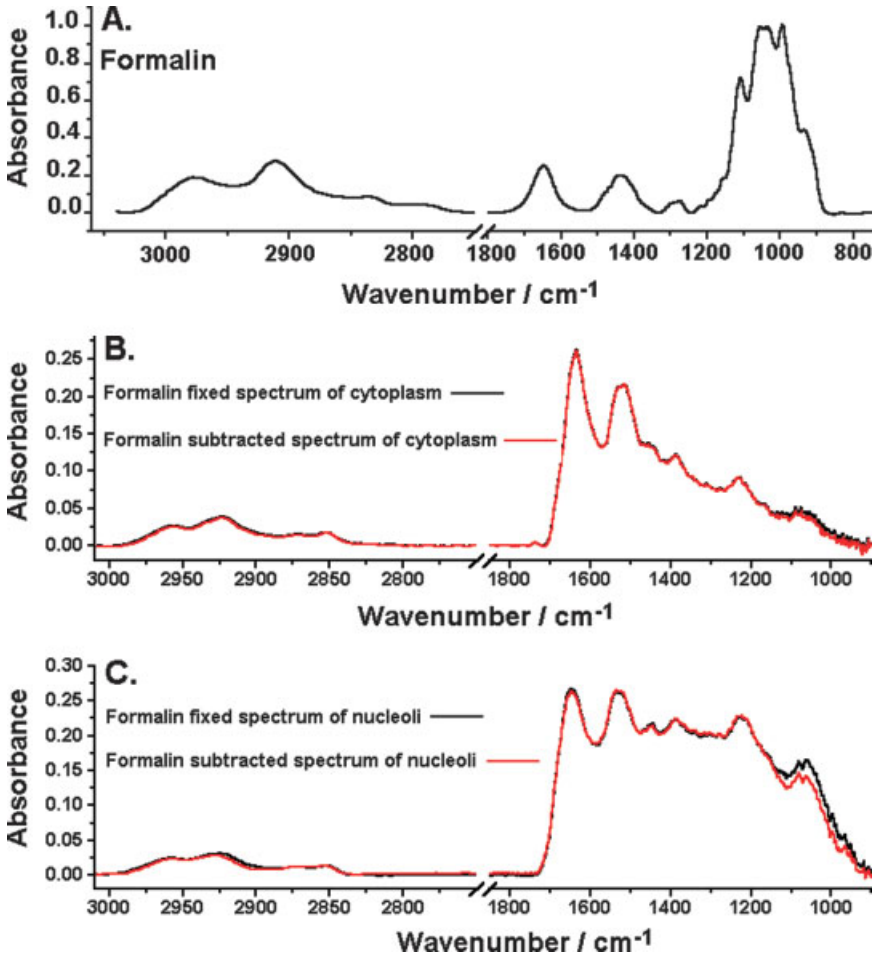

FIGURE 4 (a) The IR spectrum of formalin. Overlay of the IR spectrum of the (b) cytoplasm and (c) nucleoli (taken from the formalin-fixed PC-3 cell), with the same spectra processed to remove their theoretical formalin content.

immersions in solutions containing increasing ethanol concentrations was used to dehydrate the aqueous component of this fixative from within the cells. This process may remove lipids that have not been appropriately fixed by formalin. However, ethanol dehydration will not remove unfixed proteins since ethanol itself is a protein-crosslinking fixative.[8] The third step of the CPD process involves exposure of the cells to acetone. Acetone acts upon biomolecules in a similar manner to ethanol.[8] Thus, we would expect further leaching of unfixed lipids out of the cell, but preservation of proteins. Therefore, although the CPD process prevents structural damage in cells by avoiding surface tension forces, it may not retain all biomolecules, particularly lipids.

The trypan blue stain was used to assess the membrane integrity of the formalin–CPD fixed cells. The cells were found to be positive to trypan blue staining, indicating some loss of plasma membrane lipids (Figure 5).

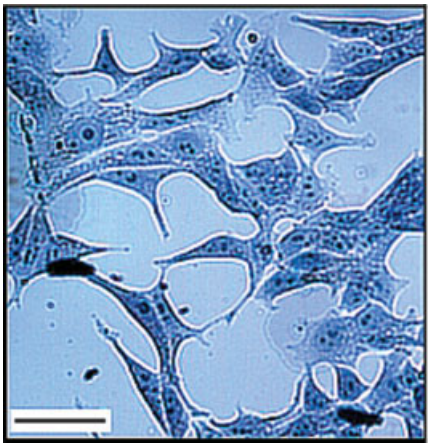

FIGURE 5 Formalin–CPD fixed PC-3 cells are positive to trypan blue staining, indicating some loss of membrane integrity. Scale bar in photomicrograph = 100 μm.

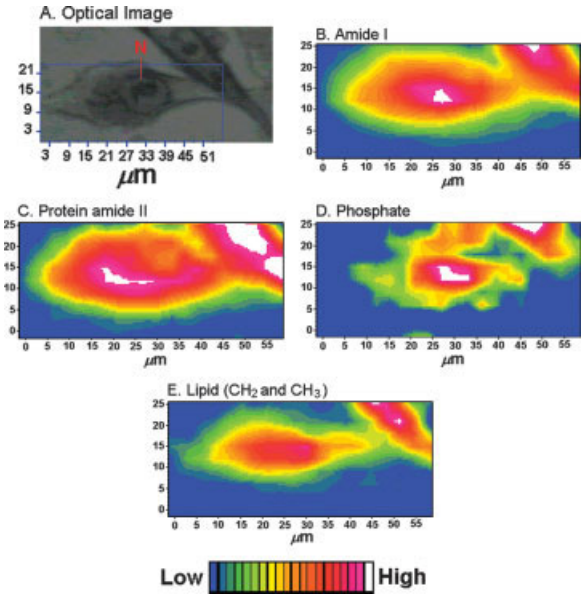

FIGURE 6 (a) Optical image of CPD fixed PC-3 cell. N designates the nucleus. Cytoplasmic areas on either side of the nucleus. Localizations and intensity profiles of (b) amide I (1721–1574-cm^{-1} peak area); (c) amide II (1568–1468-cm^{-1} peak area); (d) phosphate (1268– 1180-cm^{-1} peak area); (e) lipid (3000– 2830-cm^{-1} peak area). IR image recorded with a 7×7 μm sampling aperture at a 3-μm step size. Image acquisition time was 4 h and 54 min.

Figure 6a shows an optical image of a formalin–CPD fixed PC-3 cell. In this figure, N denotes the cell nucleus and the cytoplasm is located on either side of the nucleus. The optical image of the cell cytoplasm shows dark grey areas immediately surrounding the nucleus, which are the cell's organelles.

The intensity distribution of the amide I peak across this cell (Figure 6b) shows intense absorption in the nucleus (at 27– 39 μm; *x*- -axis), as expected, since the amide I has contributions from nucleic acids as well as proteins.[13] The amide II distribution was found to be intensely located within the dark grey areas of the cell cytoplasm, immediately surrounding the nucleus. The localization of the amide II absorbencies suggest that it may be associated with synthesized proteins, manufactured in the ER, and this conforms to the amide II localization observed in the formalin-only fixed SR-FTIR image (Figure 2c). In addition, the most intense amide II signals (white pixels in Figure 6c) are localized in areas of high cytoplasmic phosphate signal depicted by the red-orange pixels in Figure 6d. This suggests that the synthesis of proteins requires a high degree of phosphorylation activity. The intensity of phosphate signals elsewhere in the cytoplasm of the formalin–CPD fixed cell is relatively low (green-yellow pixels) and well resolved. This is because the nucleus is situated towards one end of this cell and the majority of its cytoplasm is located on one side. Thus, the area within which the cytoplasmic components can distribute is larger. This can be compared to the formalin-only fixed cell (Figure 2a), which has a large nucleus at the center of its body so that its cytoplasmic contents are distributed on either side of its nucleus, which reduces the available space for these cytoplasmic components to locate. Hence, the intensity distribution of cytoplasmic phosphate signals are less well resolved in cells that have a large nucleus to cytoplasm size ratio.

The most intense phosphate signals (white pixels) arising from the formalin–CPD fixed PC-3 cell occurs in the nucleus and conforms to observations made for the formalin-only fixed SR-FTIR image of the PC-3 cell (Figure 2d).

The lipid (CH_2 and CH_3) intensity distribution, Figure 6e, is similar to that of the amide I distribution. The high lipid (CH_2 and CH_3) intensity distribution (orange-pink pixels) suggests that the concentration of lipids detected from organelles in the cytoplasm (dark grey areas of cytoplasm in optical image) is similar to the concentration detected through the nucleus in these formalin–CPD fixed cells. This lipid intensity distribution contradicts those obtained from formalin-only fixed cells (Figures 2e and f), where the lipid intensity is higher in the cytoplasm than in the nucleus. Therefore, this result from the formalin–CPD fixed cell indicates a higher degree of leaching of cytoplasmic lipid components compared with formalin fixation without subsequent CPD. Additionally, the lipid ester (C═O) peak at ~1740–1725 cm^{-1} was not observed in the formalin–CPD fixed cell IR spectra, which also coincides with a significant loss of lipid molecules.

SR-FTIR Images of Glutaraldehyde–Osmium Tetroxide–CPD Fixed PC-3 Cell Line

Glutaraldehyde– osmium tetroxide fixed cells were negative to trypan blue staining, indicating preservation of plasma membrane lipids.

Figure 7a shows an optical image of two glutaraldehyde– osmium tetroxide fixed PC-3 cells, labeled as cells 1 and 2. The nucleus (N) and cell cytoplasm (C) are designated on this image. A cross-section through these cells was imaged by SR-FTIR microspectroscopy. As expected, the amide I distribution is observed intensely within the nucleus of both cells (Figure 7b) and agrees with observations made for the amide I intensity distributions in formalin and forma-

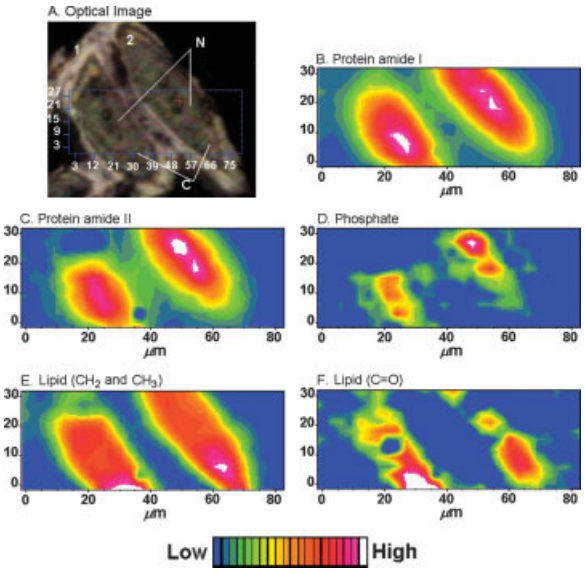

FIGURE 7 (a) Optical image of 2 glutaraldeyde–osmium tetroxide–CPD fixed PC-3 cells (labeled 1 and 2). N designates the nucleus, C designates the cell cytoplasm. Localizations and intensity profiles of (b) protein amide I (1721–1574-cm^{-1} peak area); (c) protein amide II (1568–1468-cm^{-1} peak area); phosphate (1271–1180-cm^{-1} peak area); (e) lipid (CH_2 and CH_3) (3000–2830-cm^{-1} peak area); (f) lipid ester (C═O) (1756– 1722-cm^{-1} peak area); IR image recorded with a 7 × 7 μm sampling aperture at a 3-μm step size. Image acquisition time was 5 h and 38 min.

lin–CPD fixed cell images. However, the amide II localization (Figure 7c) in the glutaraldehyde–osmium tetroxide fixed cells is similar to that of the amide I image and does not agree with observations made for the formalin-fixed cells, where the amide II was located intensely within the cytoplasm. The protein amide I and II images show absorption between the two cells, which may arise from protein actin filaments or proteins involved in cell-to-cell adhesion and or signaling.

The phosphate signal locates with high absorbance within the nucleus and conforms to observations made in formalin-fixed cell images. The lipid (CH_2 and CH_3) image (Figure 8e) shows localization with high intensity within the cell cytoplasm of each cell and conforms to images taken with formalin fixation. Accordingly, the lipid ester (C═O) image (Figure 7f) shows intense localization within the cytoplasm of both cells and a notable decrease at the nucleoli in each cell.

Figure 8a shows a typical IR spectrum derived from the glutaraldehyde–osmium tetroxide fixed PC-3 cells. Figure 8b shows the IR spectrum of glutaraldehyde. IR peaks in the spectrum of glutaraldehyde may overlap with cellular lipid (~2950– 2685, 1754, 1477–1221 cm^{-1}), amide I (~1645 cm^{-1}), and several other biomolecules between 1218 and 765 cm^{-1}. Osmium tetroxide gives rise to absorbencies at less than 1000 cm^{-1}, which does not interfere with the spectral region of interest in this study. In the images shown in Figure 7, we observe good localization of lipid, phosphate, and amide I signals, which are comparable to those obtained from the formalin-fixed cells. By means of the same procedure described in the section, SR-FTIR Images of the Formalin Fixed PC-3 Cell Line above, the most intense peak in the glutaraldehyde spectrum (at 950 cm^{-1}) was used to determine the upper limit of glutaraldehyde absorption in the glutaraldehyde–osmium tetroxide fixed PC-3 cell spectrum. The intensity of absorption at 950 cm^{-1} in the spectrum of the glutaraldehyde–osmium tetroxide fixed PC-3 cell is 0.04 AU. The glutaraldehyde spectrum was normalized to this value (0.04 AU) and subtracted from the spectrum of the glutaraldehyde–osmium tetroxide fixed PC-3 cell shown in Figure 8a. We observed no significant differences in the intensities of peaks across the glutaraldehyde–osmium tetroxide fixed PC-3 cell spectrum, when compared to the same spectrum in which the glutaraldehyde content was removed.

However, we find that the amide II signal in the SR-FTIR image of the glutaraldehyde–osmium tetroxide fixed PC-3 cells (Figure 7c) differs in localization, when compared to the amide II images obtained by formalin fixation (Figures 2c and 6c). It may be the case that the number of nucleoli is greater in the cells that were fixed by glutaraldehyde and osmium tetroxide, in which case the histone proteins in each nucleolus would contribute to amide II absorption, resulting in higher signals of amide II within the nucleus, relative to the cytoplasm.

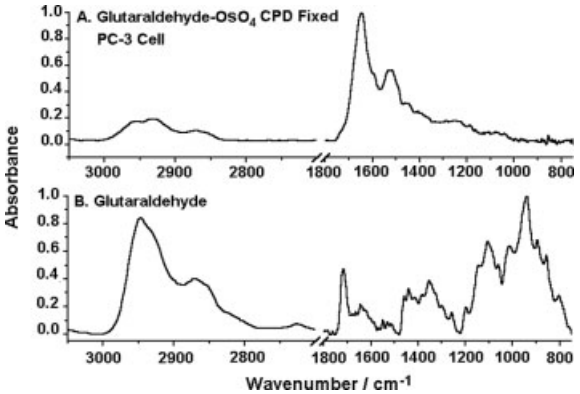

FIGURE 8 (a) The typical IR spectrum of a glutaraldehyde–osmium tetroxide fixed PC-3 cell; (b) The IR spectrum of glutaraldehyde.

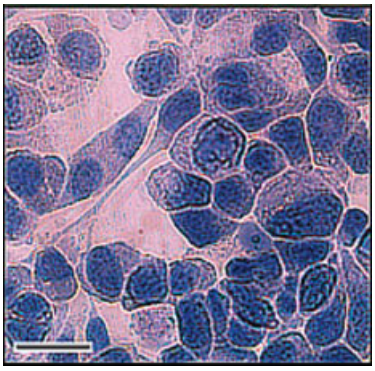

FIGURE 9 Unfixed PC-3 (PBS-centrifuged) cells are positive to trypan blue staining, indicating some loss of membrane integrity. Scale bar in photomicrograph = 50 μm.

SR-FTIR Images of Unfixed PC-3 Cell Line

A positive result of trypan blue staining of the unfixed cells was observed (Figure 9). This indicates a loss of lipids from the plasma membrane. Therefore, the centrifugation step is not appropriate for dehydrating the cells without loss of membrane integrity.

Figure 10a shows an optical image of unfixed PC-3 cells. It is difficult to locate the nucleus and cytoplasmic compartments due to an overlay of residue salt arising from the PBS treatment during sample preparation. In the optical image of the cell cluster shown in Figure 10a, we use the cell marked with an arrow to discuss the localizations of various IR signals within the unfixed cell. We observe in Figures 10b and 10c that the amide I and II intensities are localized at high intensities (white pixels) at the same location [at coordinates (40 and 55 μm)] within the cell. We may assume that this intense amide I localization may arise from the nucleus, and the intense amide II signal may be localized at this location due to absorption arising from histone proteins of multiple nucleoli. However, processing of further SR-FTIR images of unfixed cells revealed that the amide II signal consistently localized with the amide I signal.

The phosphate signal (Figure 10d) shows intense localization at the region of intense amide I signal, which may confirm this location [at coordinates (40 and 55 μm)] as the nucleus. However, the intensity of phosphate signal in other parts of the unfixed cell is fairly homogenous when compared with the phosphate distributions in formalin-fixed (Figures 2d and 6d) and glutaraldehyde–osmium tetroxide fixed cells (Figure 7d). The homogenous phosphate signals observed in the unfixed cells may arise as a result of phosphate absorption from the PBS residue on the surface of the cells.

The lipid (CH_2 and CH_3) signal (Figure 10e) shows intense localization (white pixels) in a region outside the speculated nucleus. This intense lipid (CH_2 and CH_3) signal is distributed in an elongated fashion and may arise from the membranes of the ER and/or Golgi apparatus within the cytoplasmic compartment. The most intense lipid (C═O) signal (Figure 10f) localizes at the speculated nucleus and does not localize with the intense lipid (CH_2 and CH_3) signal as observed in our fixed cells. The lipid (C═O) signal is observed as a homogenous distribution of intensity across the unfixed cell and cannot be used to locate organelles.

CONCLUSIONS

We have studied the effects of cell fixation on the localization of various biomolecules by SR-FTIR microspectroscopy. The formalin-fixed cells revealed differences in the intensity distribution of lipids across the cell, when compared to formalin–CPD fixed cells.

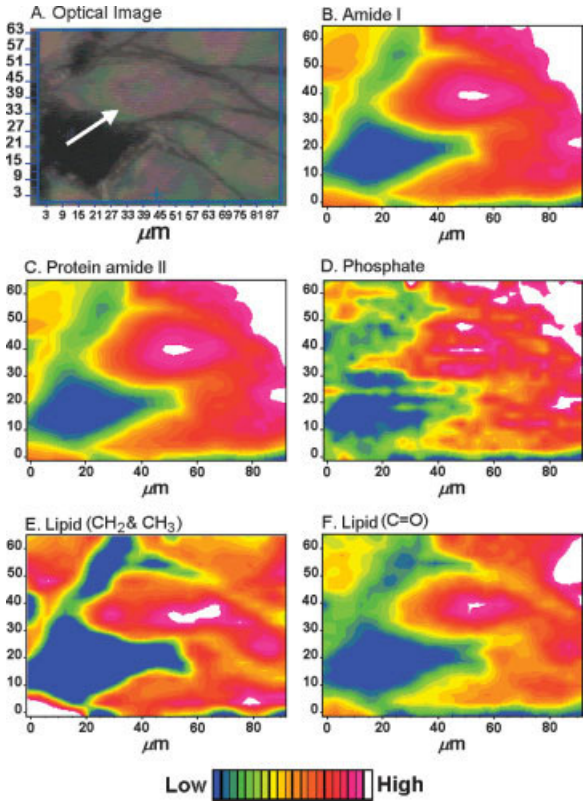

FIGURE 10 (a) Optical image of unfixed (PBS -centrifuged) PC-3 cells. The cell labeled with an arrow is discussed in detail within the text. Localizations and intensity profiles of (b) amide I (1721–1574-cm^{-1} peak area); (c) protein amide II (1572–1473-cm^{-1} peak area); (d) phosphate (1268–1180-cm^{-1} peak area); (e) lipid CH_2 and CH_3 (3000–2830-cm^{-1} peak area; (f) lipid (C═O) (1756–1722-cm^{-1} peak area). IR image recorded with a 7 × 7 μm sampling aperture at a 3-μm step size. Image acquisition time was 8 h and 34 min.

The formalin-fixed cells exhibited greater lipid localization in the cells cytoplasm than in the nucleus [most clearly depicted by the lipid ester (C═O) signal], whereas the formalin–CPD cell showed similar localizations of lipids in the nucleus and cytoplasmic areas close to the nucleus. Thus, formalin fixation alone preserves a greater amount of cytoplasmic membranous components than formalin–CPD fixation, which involves the use of the lipid leaching solvents, ethanol, and acetone. Additionally, the formalin-fixed cell IR spectrum exhibited the lipid ester (C═O) peak, which was not observed in the spectrum derived from the CPD processed cell and confirms a significant loss of lipids using the CPD technique.

The contribution of formalin to the IR spectrum was not significant. This was confirmed by the localizations and intensity profiles of functional group vibrations corresponding to the phosphate, lipid, and protein domains in regions of the cell where we would expect these molecules to arise. In addition, we have shown that the IR spectrum of the formalin-fixed cell demonstrates no significant differences in peak intensities when compared to the same spectrum with formalin removed.

Using the prostate cancer PC-3 cell, we have demonstrated that it is essential to use all of the available spectral information to elucidate subcellular domains within the cell. This required a sampling aperture size that provided good S/N IR spectra without compromise to spatial resolution.

The SR-FTIR images of formalin-fixed cells exhibited better localization of biomolecular domains (lipid, phosphate, and synthesized proteins), when compared to unfixed cells, although both types of fixation demonstrated some loss of plasma membrane integrity. The unfixed cells might provide better localizations of phosphate signal if a washing step were employed prior to centrifugation to remove the residue PBS from the surface of the cells.

The glutaraldehyde–osmium tetroxide–CPD fixed cells revealed similarities with the formalin-fixed cells regarding the localizations and intensity profiles of the amide I, phosphate, lipid (CH_2 and CH_3), and ester (C═O) signals. Thus, although the formalin-fixed cells exhibited a loss of membrane integrity (evident through trypan blue staining), the retention of biomolecular domains and intensity of signals at these locations is not effected to a degree that is apparent in the SR-FTIR image. Therefore, formalin fixation, which is a simpler and a considerably less time-consuming method of sample preparation than glutaraldehyde–osmium tetroxide–CPD fixation, can be used to provide highly resolved biospectroscopic images of subcellular chemistry within cells.

In conclusion, formalin cell fixation can play an important role in future applications of FTIR-based biomechanistic studies, in vitro, since the molecular structure of the cell is maintained and the resulting IR data can be interpreted with greater confidence with respect to the specific mechanism under study since consequences arising from the activation of necrosis pathways are avoided. The use of cell fixation using formalin may facilitate the establishment of FTIR microspectroscopy as an important tool in the analysis of chemical composition within cells or tissue, whose structure and morphology is preserved.

We acknowledge EPSRC for financial support (E. Gazi). We gratefully thank Dr. Mark Tobin (Daresbury Laboratory, UK) for help during SR-FTIR measurements.

REFERENCES

1. Reffner, J. A.; Carr, G. L.; Williams, G. P. Mikrochim Acta Suppl 1997, 14, 339–341.
2. Holman, H. Y. N.; Bjornstad, K. A.; McNamara, M. P.; Martin, M. C.; McKinney, W. R.; Blakely, E. A. J Biomed Opt 2002, 7(3), 417–424.
3. Dumas, P.; Jamin, N.; Teillaud, J. L.; Miller, L. M.; Beccard, B. Faraday Discuss 2004, 126, 289–302.
4. Jamin, N.; Dumas, P.; Moncuit, J.; Fridman, W. H.; Teillaud, J. L.; Carr, L. G.; Williams, G. P. Proc Natl Acad Sci USA 1997, 95, 4837–4840.
5. Lasch, P.; Boese, M.; Pacifico, A.; Diem, M. Vib Spectrosc 2002, 28, 147–157.
6. Lasch, P.; Pacifico, A.; Diem, M. Biospectroscopy 2002, 67, 335–338.
7. Tobin, M. J.; Chesters, M. A.; Chalmers, J. M.; Rutten, F. J. M.; Fisher, S. E.; Symonds, I. M.; Hitchcock, A.; Allibone, R.; Dias-Gunasekara, S. Faraday Discuss 2004, 126, 27–38.
8. Kieran, J. A. Histological and Histochemical Methods: Theory & Practice; Pergamon Press, Oxford, UK, 1990; Chap 2.
9. Stoward, P. J. Fixation in Histochemistry; Chapman and Hall: London, 1973.
10. Smith, M. E.; Finke, E. H. Invest Ophthamol 1972, 11(3), 127–132.
11. Gamliel, H. Scan Elec Microsc 1985, 4, 1649–1664.
12. Kaighn, M. E.; Narayan, K. S.; Ohnuki, Y.; Lechner, J. F.; Jones, L. W. Invest Urol 1979, 17, 16–23.
13. Chiriboga, L.; Xie, P.; Yee, H.; Vigorita, V.; Zarou, D.; Zakim, D.; Diem, M. Biospectroscopy 1998, 4, 47–53.
14. Diem, M.; Chiriboga, L.; Yee, H. Biopolymers 2000, 57, 282–290.
15. Alberts, B.; Bray, D.; Lewis, J.; Raff, M.; Roberts, K.; Watson, J. D. Molecular Biology of the Cell; Garland Publishing: New York, 1994; Chap 12.

Reviewing Editor: Dr. Laurence A. Nafie